

PAPER • OPEN ACCESS

Wear Behavior and Mechanism of CoCrMo Alloy Fabricated by Powder Metallurgy Route

To cite this article: Muna Khethier Abbass and Jawdat Ali Yagoob 2019 *IOP Conf. Ser.: Mater. Sci. Eng.* **518** 032009

View the [article online](#) for updates and enhancements.



IOP | ebooks™

Bringing you innovative digital publishing with leading voices to create your essential collection of books in STEM research.

Start exploring the [collection](#) - download the first chapter of every title for free.

Wear Behavior and Mechanism of CoCrMo Alloy Fabricated by Powder Metallurgy Route

Muna Khethier Abbass¹ and Jawdat Ali Yagoob²

¹Dept. of Production Engineering and Metallurgy, University of Technology, Baghdad, Iraq

¹mukeab2014@yahoo.com, ²jaw2096@yahoo.com

Abstract. This research is devoted to study the wear behavior and mechanism of CoCrMo alloy due to the utilization of the alloy in application mainly exposed to wear. Samples fabricated by powder metallurgy route compacted under (1000MPa) and sintered at (1200°C) in the argon atmosphere. Wear test type pin-on-disc was performed under dry sliding condition over steel counterface disc. For the first group of wear tests four vertically loads (10,15,20 and 25) N were applied at fixed sliding speed (1.476) m.s⁻¹, time (15 min) and sliding distance (1329m). The second group of tests were conducted at fixed applied load (25) N for (60 min) interrupted to four equal intervals and at the same above sliding speed. The worn surface of the tested samples and formed wear debris particles were investigated and analyzed with aid of SEM and SEM-Mapping facilities. The results showed that the wear rate increased by increasing the applied load and a transition from mild wear to severe wear was occurred at (20 N) for fixed sliding time (15min). The maximum measured wear rate was (39.72×10⁻⁷) mm³.mm⁻¹ at the highest applied load. While for the second group the wear rate was decreased when the sliding time exceeded 30 min. The main wear mechanism was adhesive type detected by material transfer, with lower abrasive type which is revealed from the existence of fine grooves. Oxidation and plastic deformation features are also observed.

1. Introduction

Wear is the surface failure that limits the use of metallic implant. Proper material election avoids the catastrophic wear (Quickly happening or accelerating surface destruction as defined by ASTM standard-G40) [1].

William et al. [2] referred to that the wear of materials is governed by the tribo-system conditions and factors such as wear mechanisms and rate, conversion between steady-state and prime wear, generation and geometry of wear debris all are important key factors. When these factors are not reported, it is difficult to compare wear data found with different protocols. Reza [3] referred to the information that was reported by (Harman, 1997) who was informed that altering implant material from UHMWPE to CoCrMo alloys (CCMAs) substantially diminishes the formation of debris in knee joint replacement. However, MITSUO [4] stated that when the need is good anti-wear biomaterial, CCMAs is well attended. Several researchers used pin-on-disc technique (PODT) in their concerned works about biomaterials. This may return to that in (PODT) after run-in, surface pressure remains constant, easy to determine the volume and rate of the wear as Mohamed et al. [5] pointed out. Qingliang et al. [6] investigated the tribological properties of a coated by plasma nitriding process and uncoated cast CCMA by (PODT). The adhesive wear was the main mechanism for both types. The improvement of wear resistance of nitrided CCMAs is attributed to the formation hard CrN and Cr₂N compounds on the surface. Bedolla et al. [7] assessed the wear resistance of alloy by (PODT). It was found that the best wear resistance was provided by a microstructure with minor grain size without main effect of type of structure; either it is either FCC or HCP. In turn Kenneth et al. [8] investigated in vitro wear resistance



of two different carbon content CCMA's by (POD) tests. The alloy with carbon content (0.25%) presented the best resistance. Akihiko et al. [9] analyzed the wear resistance of forged and cast alloys with (0.067 and 0.26) %C respectively by (PODT). The results showed that the cast samples were worn much more than the forged ones. The attribution was owing to the formed coarse precipitation of carbides during solidification which contributed to increase abrasive wear. While the forged samples free of carbides with finer grain sizes showed better resistance, particularly to fatigue wear type. Varano and colleagues [10] found that the samples made from ASMT F75 with larger carbides have the most damaged features, since the carbides were tearing away and generated abrasive wear. Thus, they suggest that the carbides may not be active in defensive against abrasion and in applications where there is formation of an oxide layer of the same material, as in these alloys. Therefore, they have considered that the key to lowering wear is simply the amount of dissolved carbon in the FCC matrix by inhibition the transition to HCP. However, a few attempts and tests were done under dry sliding situations [4]. Zhao et al. [11] tested as-sintered cylindrical samples made from Co-30Cr alloys under dry sliding at room and 600°C temperatures. They used firstly a disc made of stainless-steel type 440C as counterface, then alumina ball to perform their experiments. No debris was generated at first case, while sliding against alumina ball tend to more debris generation with sizes (up to ~ 200 µm) at 600°C, and lower amount at RT with sizes (up to ~ 80 µm). Chemical compositions of the debris at both temperatures are the same and both composed of Co, Cr, Al and O. Saldívar-García et al. [12] studied the wear of wrought and cast CCMA's, under dry sliding using a (POD) tribometer. They found an important effect of the microstructural structures on the alloy wear and the least volume wear losses were reached in HCP-HCP (POD) pairs. While the highest values were corresponded to FCC-FCC pairs. The FCC-HCP pairs showed the intermediate losses. Dong Mua et al. [13] investigated the mechanisms due to the dry sliding of CCMA with a ring-on-block technique at 950°C. The ring made of steel type GGr15 (HRC52). The wear resistance of the boronized CCMA was better than unboronized one due to the higher surface hardness of the boronized CCMA. Even with outstanding biocompatibility and dependable tribological behavior, however, wear and friction problems are still continual for CCM/CCM pair as referred by Chi-Wai [14]. From the studies that were reviewed not necessarily all of them are referred to them in the present research which were related to the wear phenomena of CCMA's it was found that most of them related to the cast or wrought types of CCMA's. Other researchers were focused their attempts on the tribocorrosion property of the alloy, because of their interest in the behavior of the alloy as a biomaterial, although the alloy also has industrial applications. Nevertheless a few works have been studied the dry sliding wear of the alloy such as Ali et al. [15]. But unfortunately, none of them covered more than one assessing factor of wear phenomena. This factor was the determination of wear rate. From these gaped knowledges about the fabricated of the CCMA's by PMR. The present research is devoted to studying the wear behavior and mechanisms of CCMA fabricated by (PMR) in a somewhat border case including wear rate assessment under variable load and fixed load besides investigation of the worn surface features and the analysis of generated wear debris were performed. Therefore, the present research will be an attempt to cover the lack to the detailed works related to wear behavior of the CoCrMo alloys under dry sliding condition.

2. Experimental methodology

2.1. Material

Pre-alloyed spherical shape CoCrMo alloy (CCMA) powder was used. It was supplied by China Jingan Chemicals & Alloy Limited Company. Table1 shows the chemical composition of as received powder and X-ray fluorescence (XRF) technique analyses which performed by Uniqe-Tech company-Turkey using Bruker S8 Tiger XRF spectrometer.

Table1. Chemical composition of as received powder CoCrMo alloy

E (wt%)	Co	Cr	Mo	Si	Mn	O
A	Bal.	28.52	5.95	—	—	0.035
B	62.97	29.2	6.612	0.38	0.319	—

E: element, A: Standard value by company specification, B: Measured value by XRF analysis

This powder was used to prepare the dry sliding wear tests samples. The samples were fabricated by powder metallurgy route. The average particles size was $47.983\ \mu\text{m}$ and 3 wt% stearic acid was added as a lubricant to CCMA powder. The route was accomplished firstly by cold compaction with an application of (1000) MPa followed by sintering for 2 hrs at 1200°C under argon atmosphere from the beginning to the end of the sintering process. The heating rate is fixed at $10^\circ\text{C}/\text{min}$. The furnace (type CARBOLITE-UK) switched off and the samples left to cool slowly inside it. The parallel face of the 10 mm cylindrical samples was wet ground using silicon carbide emery papers with (240, 600, 1000, 2000 and 3000) grit then polished using $5\ \mu\text{m}$ alumina suspension solution, washed with distilled water and dried in laboratory oven type LHT/60-UK at 120°C for half an hour. Vickers micro-hardness for compacts was measured by Metkon microhardness tester with 500 gm applied the load in Mechanical Engineering Department laboratory-Tikrit University. The average value of the five readings was (335 HV). Optical microscopy using invert trinocular microscope type OPTIKA-Italy and SEM instrument type (VEGA3LM TESCAN COMPANY) provided with EDS (type Oxford) were used for microstructure, worn surface and wear debris observation and analyses.

2.2. Wear tests

First of all, the roughness of the exposed surface of wear test samples were measured by surface roughness measuring instrument type Pocket Surf[®] portable surface roughness gages / Mahr Federal USA. The measurement was done using 0.75 mm cut-off length with 1 sampling length and the test was repeated for additional two times. The calculated average of the three reading of the arithmetical mean deviation (Ra) was ($0.316\ \mu\text{m}$) with standard deviation ($S = 0.0351$). All tested samples were dried in an electric oven at 120°C for half an hour then slowly cooled inside it to ambient temperature, thereafter covered carefully with layers of dried cloth then kept inside moisture free plastic container finally deserted directly before the wear test. It is important to clarify that because of the significant effect of the moisture that is absorbed into the samples from the open pores at their surface and this will effect on the value of the initial mass of the samples before the test. Hence, the removing of the moisture by drying is very important factor for accurate measurement of the mass loss due to dry sliding. This procedure was done deepening on the personal experience. EN31 steel counterface disc with 62 HRC (746 HV) was ground by (1000 and 2000-grit silicon carbide) emery paper then cleaned with acetone before and after each wear test and dried with a stream of hot air. Wear tests were performed under dry sliding condition by using pin-on-disc tribometer according to ASTM: G99, type (Ed-201 wear and friction monitor)/Ducom Make, India. Figure 1 represents a photograph for the used tribometer. All experiments were conducted at temperature ($33\pm 1^\circ\text{C}$) which is referring to the ambient temperature when the tests were performed. The tests carried out in two groups. The first group includes four samples which were tested for fixed time (15 min) and under different applied loads (10, 15, 20 and 25) N. The second group was performed under fixed applied load (25 N) for discontinuous (60 min) test period. Here also the mass loss was weighted after each (15 min).



Figure 1. A: Pin-on-disc tribometer, type (Ed-201 wear and Friction, monitor), B: Measuring of contact temperature, C: Example for a measured temperature value.

Each sample was weighted by sensitive digital balance type Sartorius-Germany with 0.1 mg accuracy directly before and after wear test to obtain (W_0) and (W_1) respectively. The stationary pin located vertically on the rotating counterface surface. Wear rate was calculated by using the following relationship [16 ,17]:

$$\Delta WR = W/S \rho_{pr} \quad (1)$$

$$S = V \times t \quad (2)$$

$$V = 2 \pi r n \quad (3)$$

$$\Delta W = W_0 - W_1 \quad (4)$$

Where: WR: Wear rate cm^3/cm , S: Sliding distance 1.329×10^6 cm, V: Linear sliding velocity 1.4765 m.s^{-1} , W_0 : Weight of unworn samples (g), W_1 : Weight of samples after the test (g) , r: Sliding radius 30 (mm) (From the center of the disc to the center of the sample) , n: Sliding speed 470 (r.p.m), t: Sliding period 15 (min), ρ_{pr} : Practically measured density of CoCrMo alloy 7.16 gm/cm^3

Note that all units have been consolidated upon compensation in the relevant laws in order to obtain the rate of wear in mm^3/m unit. The temperature at nearby points to the contact region between the CCMA samples and counterface surfaces are measured by using portable infrared thermometer type Aswar as explained in the figure 1-B and C. In other hand generated wear debris from the wear test of the second group was collected and observed with SEM. Because the 60-min test period for the second group is enabled to get an adequate amount of debris particles.

3. Results and Discussion

3.1. Microstructure of CCMA

Figure 2 indicates the microstructure of CoCrMo alloy (CCMA) after etching using etching solution prepared from (60 ml HCl, 15 ml HNO_3 , 15 ml acetic acid and 15 ml distilled water) [15]. It explains the formation of the microstructure from two main phases, an electronic compound with dendrite like shape phase consisted only from Co and Cr elements as detected by SEM-EDS analysis shown in figure 3. While Figure 4 shows SEM-EDS analysis for etched microstructure at the matrix at other point. This image confirms the chemical composition of the used CCMA powder.

Although a continuous stream of argon gas was supplied into the cavity at which the samples were set during the whole interval of sintering, but oxidation of Cr element was happened. The analyzed point in figure 5 shows the Cr_2O_3 formed at particle boundaries region. This oxide formation also reported by Dourandish et al. [18] although they conducted the sintering under argon atmosphere.

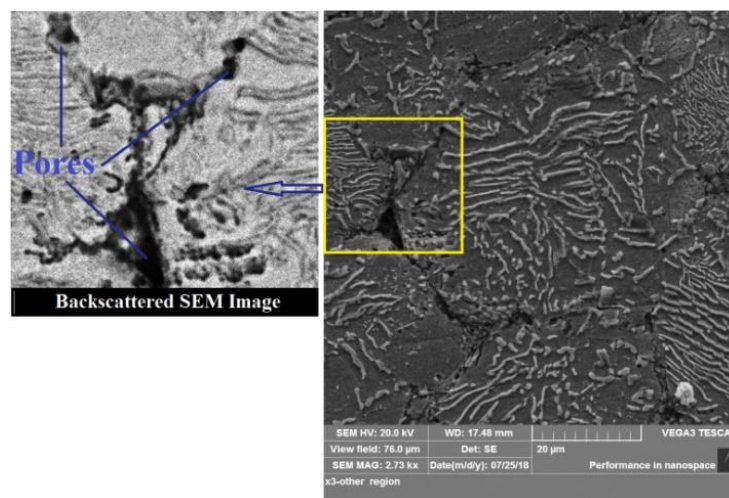


Figure 2. SEM image for etched microstructure of the CCMA sample sintered at 1200°C for 2 hrs.

The reason of Cr_2O_3 formation can be interpreted as Cr atoms migrated toward the boundaries due to driving force initiated from restricted or penetrated oxygen into pored zones at these boundaries which acted as a magnet attracted Cr atoms and form the more stable less free energy oxide with oxygen atoms which enhanced and accelerated at the sintering temperature.

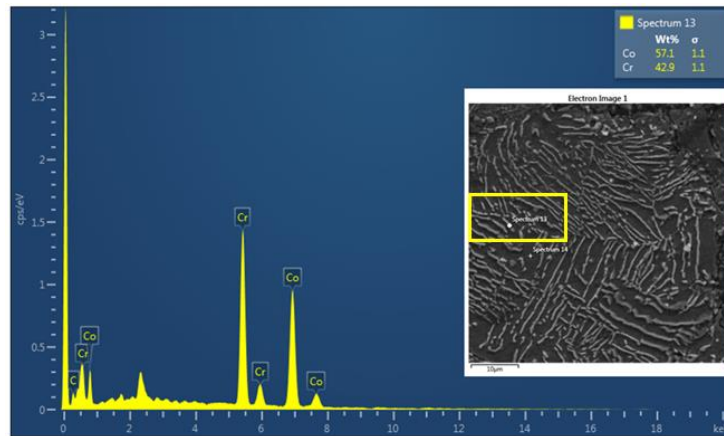


Figure 3. SEM-EDS image for etched microstructure of the sample sintered at 1200°C for 2 hrs at dendrite arm.

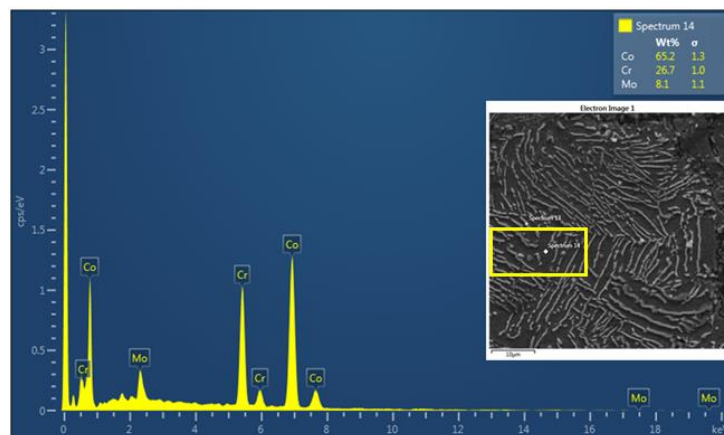


Figure 4. SEM-EDS image for etched microstructure at the matrix of the sample sintered at 1200°C for 2 hrs at other point.

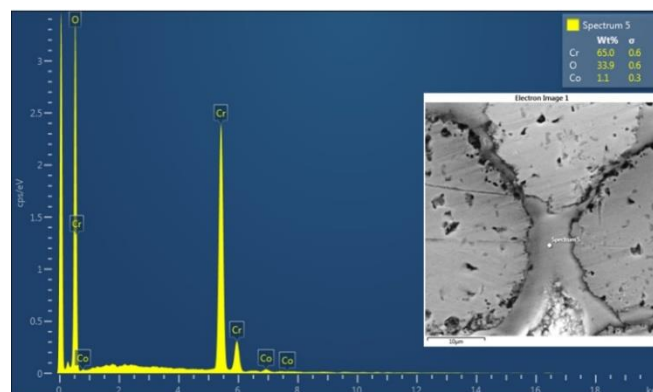


Figure 5. Back scattered SEM -EDS image for sample sintered at 1200°C for 2 hrs at other point.

3.2. Wear rates

The relationship between applied load and wear rate (WR) indicated in the figure 6 which shows three main regions. The first denotes to mild wear with low (WR) when (10 N) was applied, then it was increased with the applied load increase to (15 N), after which the rate showed relatively steady state manner in the second region within the range (15-20) N. This is evidence to the sample surface somewhat retention of its resistance to the tangential friction force although application of 5 extra newtons over applied 15 newtons. Several logical reasons may contribute to the interpretation of this manner. One of it is due to the oxidation that starts at the pin surface layer which reflected in the relative stability of (WR). Thurner et al. [19] reported the oxidation of chromium even at room temperature. Therefore, the measured increase in the temperature at a point close to the contact region due to the increase of the applied load as illustrated in the figure 7 was assistant factor for further oxidation of the surface of the samples during sliding.

The second is due to the fracture of the interrupted wear debris to smaller size which plays a role as interface layer between the pin and counterface surface for some intervals during dry sliding, before spalling out. Hence exclude the direct metal to metal contact to some extent which appears as the steadiness of the wear rate within the (15-20) N applied load range. The third region started by increasing the applied load to (25 N) which led the wear rate to increase to its greatest value. This has happened because the formed tangential force due to (25 N) application was capable to overcome the strengthening induced γ to ϵ phase transformation and also continuously removing of the formed debris from the oxidized surface layer by fragmentation outward from the contacted region. Amit Aherwar et al. [20] also observed the gradual increase of wear rate of cast Co30Cr4Mo if the (POD) tests load increased from (5 to 25) N under wet and dry conditions. The second group of wear tests was performed in order to detect the effect of sliding period at constant applied load. Figure 8 reveals that the rate of wear was increased when the test was extended to a further (15 min).

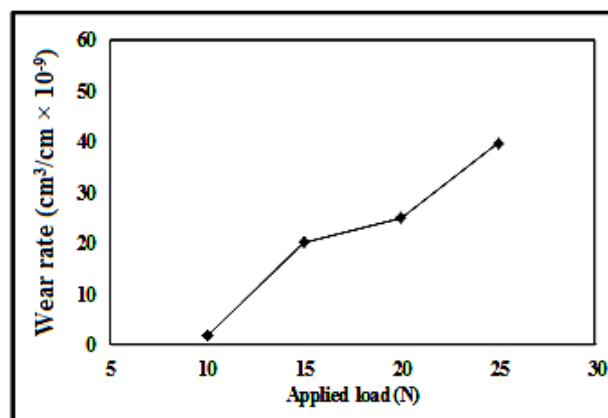


Figure 6. Dry sliding wear rate for sintered CCMA under different loads tested by (PODT) for

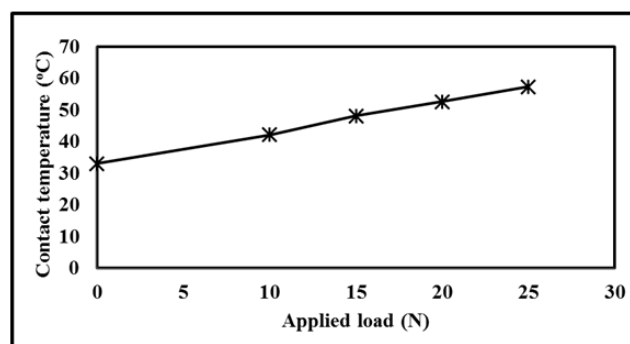


Figure 7. Temperature variation during dry sliding under 25 N for 60 min.

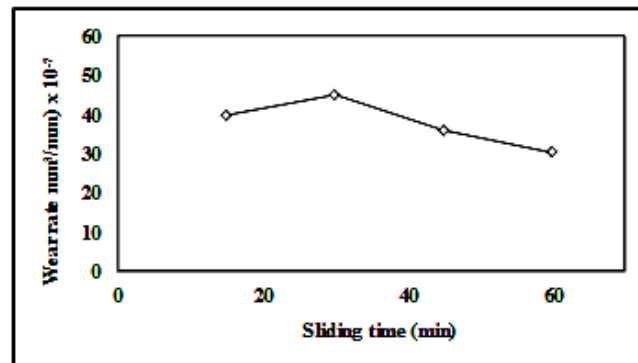


Figure 8. Dry sliding wear rate for sintered CCMA under applied load of 25 N.

This denotes to the continuity of the same behavior of the sliding couple at the first (15 min) under the same (25 N) applied load, which means also continuity of wear debris formation due to the same former explained reasons. While a further extension of test interval to reach a totally (60 min) was led to relative decreased (WR) under the same conditions. The reason could be due to running in generated deformation or strain-induced induced γ -FCC to ϵ -HCP phase transformation. This is because of CCMA susceptible to this type of transformation which enhances the twins creation. Accordingly, these actions will influence the tribological manner CCMA [4, 20].

The renewable oxidation of the pin surface associated with material transfer between the sliding couple surfaces was changed the chemistry of the surface then its behavior under dry sliding. This is reflected in the formation of wear debris with lower trend which was assessed as a decrease in (WR). Saldívar-García et al. [12] proved that the foremost mechanism for cast and wrought CCMA tested by (POD) was some plastic deformation on the contacting surfaces and it included some oxidation of the wear debris.

3.3. Worn surfaces features

Figure 9 illustrates the worn surface of CCMA resulted due to dry sliding under (25 N) applied load after (60 min). The almost adhesive wear for which the surface was exposed because of material transfer, besides oxidation left a surface with dark color. The worn surface of CCMA showed during a sliding motion, chemical bonds between its surface atoms with the mating counterface material (particularly with iron atoms). This may give rise to adhesive forces [21]. This adhesion can be assessed by the major atoms conjoint solubility. Actually, there is a degree of solubility between (Co and Fe) which reflected in the ability of Fe atoms to transfer to the surface of the pin. Also bit appearances of the fine grooves parallel to the direction of sliding refer to the abrasive wear [22].

The surface was exposed to the combination of plastic deformation and plowing action generated from the asperities of the steel counterface. The existence of rippled edges like lines indicates the plastic deformation of the surface in some positions. In other hand the reminder of fractured debris on the surface of the worn sample as shown in Figure 9 are appeared as white particles which is a strong evidence for the interpretation of the wear rate decrease which is discussed in the paragraph 3.2.

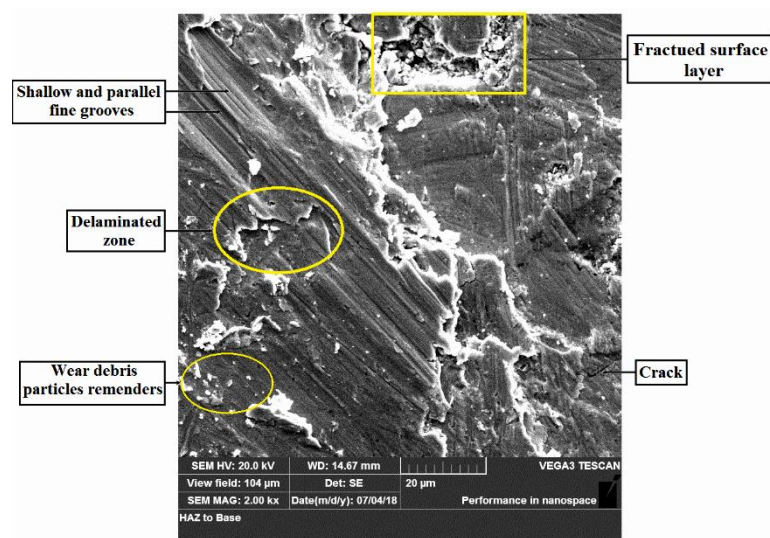


Figure 9. SEM-image for sintered CCMA worn surface appearance after dry sliding for 60 min under applied load of 25 N.

3.4. SEM- EDX-Mapping Images

Positions on the worn surfaces were analyzed with the aid EDX Mapping facility detected what really was happened from the point view of surface chemistry. Figure 10 defines the occurrence of the material transfer phenomena. The Fe element was more distributed at the left hand of the mapped area on the pin surface shown in the image tend to iron oxide formation because of a chemical reaction on a wearing surface [23]. The iron oxide formation is enhanced from the existence of O_2 at the worn surface of the pin and frictional heat energy. This oxide in turn hides the real surface of the alloy from direct contact the decrease of detected Co element at the left hand on the mapped position shown in figure 10 ensure the opinion of pin surface oxidation. The non-homogenized Fe distribution on the worn surface reveals the dynamical variation of the pin surface topography because of the more than one wear mechanism contribution, which led to occurrence of the contact action in varying degree from position to another one on the pin surface against the steel counterface and dynamically wears debris generation and removal.

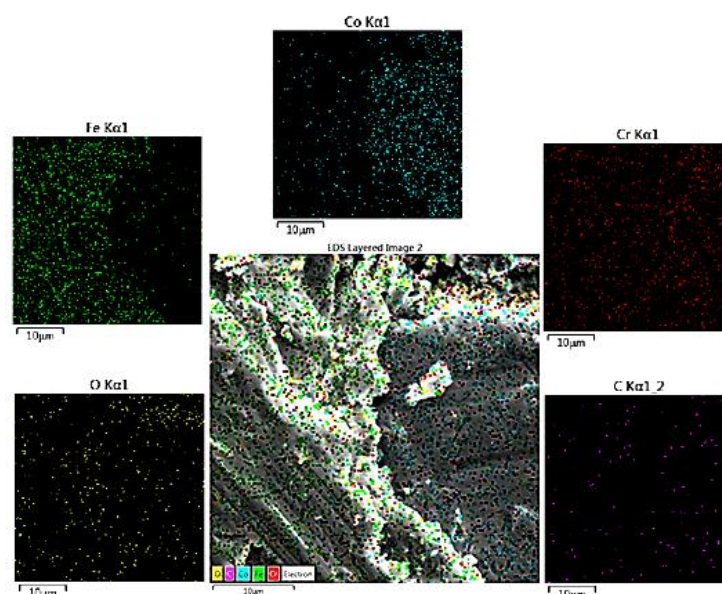


Figure 10. EDX-Mapping analysis for sintered CCMA worn surface appearance after dry sliding for 60 min under 25 N load.

3.5. Wear debris analysis

The mechanism of material removal was occurred by fragmentation of formed oxide layer formed on the surface during the process because of usually these oxides have shear strengths differ and lower from those of the alloy worn surface [24]. These oxides flake away as debris due to tangential created forces. Saldívar-García et al. [12] referred to some oxidation of the formed wear debris due to the worn of CCMA. The shapes shown in figure 11 of the detached and fragmented wear debris from the surface are simulated to some extent the two-dimension view of original particles shape after sintering with their size around ($\sim 50\text{ }\mu\text{m}$) and others with lower sizes. However, its thickness was arranged from thinned to thicker ones. The figure 11 shows some debris particles with ($\sim 10\mu\text{m}$) thickness and others with lower value. Also, the surface of the particles appeared in the same manner as the original worn surface from which they were delaminated, from the viewpoint of topography and color when comparing the two figures 9 and 11 particularly for the front face of the debris particles denoted by (F) in figure 11. While the rare surface showed a rupture like configuration as denoted by (R). Indeed, deeply observation of the shape of the detached debris particles indicates the initiation of micro-cracks then evolved into large cracks and propagated from CCMA particles boundaries (PBs) at the surface and sub-surface regions inward to CCMA particles as indicated in the figure 12, besides those initiated and propagated micro-cracks at subsurface layers beneath the sliding surface within the bulk material of the particles of the pin.

After the connection of those networks of cracks and due to tangential force during sliding, parts of the surface were fragmented as the debris illustrated in Figure 11. Indeed, the reason of some micro-cracks initiate and propagate from CCMA (PBs) can be return to the nature of the material forming the CCMA pin. The pin is consisted from CCMA particles separated by Cr_2O_3 layer as shown in figure 5. This is classified as a ceramic material. Hence it is more brittle than CCMA particles, also the bonding between those particles and interface oxide is a mainly cohesive type and it is not able to form any type of primary bonding between them. This case is reflected as a default (some weakness but not high) at (PBs). In another hand, some remained porosity between the CCMA particles after sintering which act as favor sites for cracks to initiate and propagate. Therefore; the probability of debris formation will start from (PBs) beside subsurface zone as the figure 12 clearly proves this interpretation.

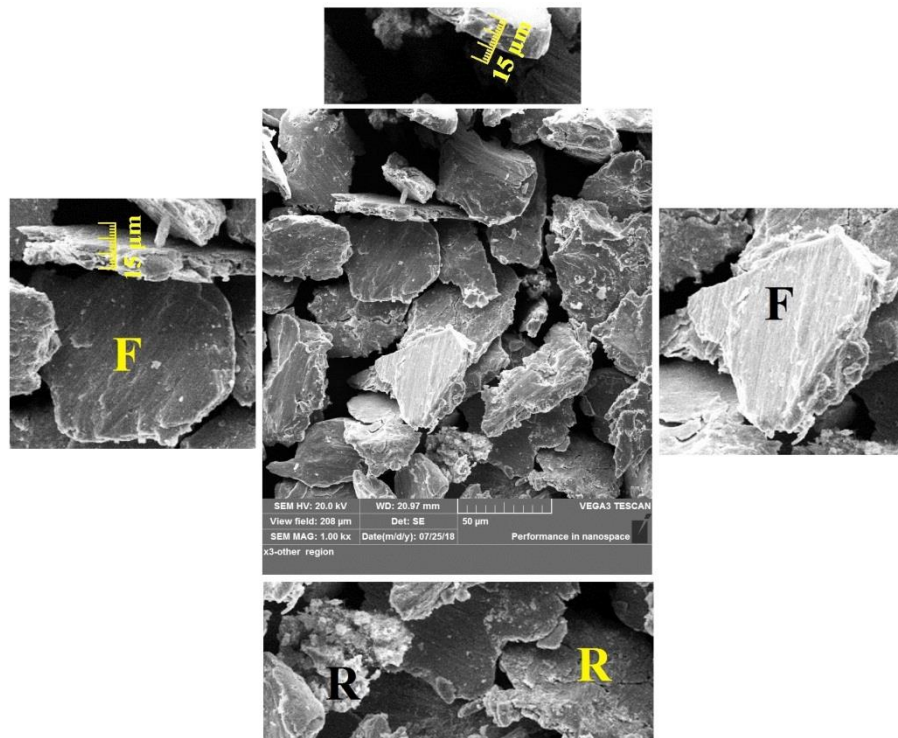


Figure 11. SEM-image for wear debris particles formed after dry sliding of sintered CCMA for 60 min under applied load of 25 N.

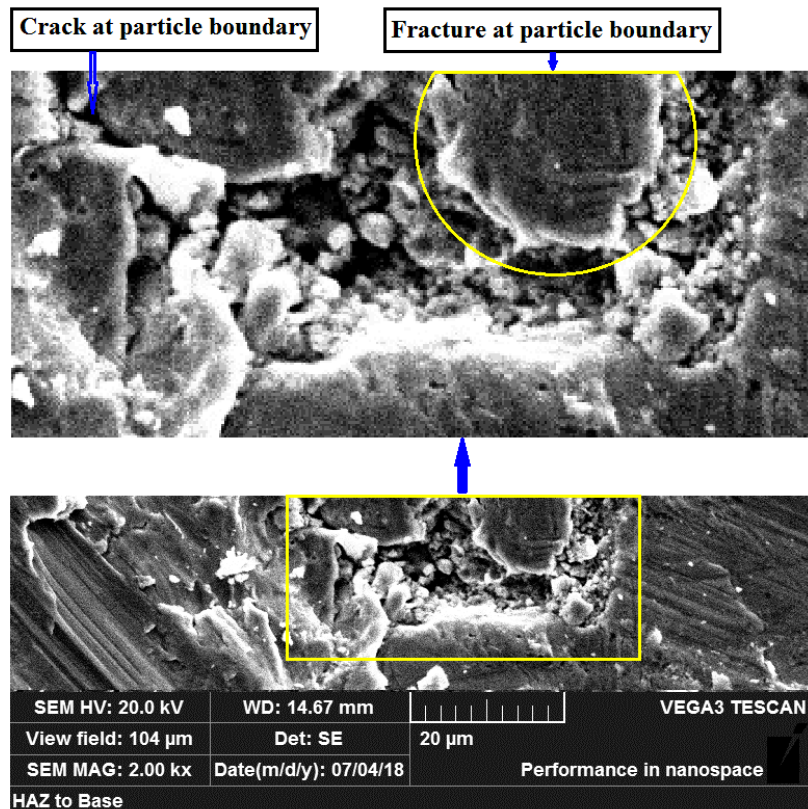


Figure 12. Magnified explanation SEM-image for the upper portion for sintered CCMA worn surface after dry sliding for 60 min under applied load of 25 N displayed in the Figure 9.

4. Conclusions

The wear behavior and mechanisms under dry-sliding of CoCrMo alloy fabricated by powder metallurgy route (PMR) were studied. The maximum measured rate was $(39.72 \times 10^{-7}) \text{ mm}^3.\text{mm}^{-1}$ at the highest applied load (25N) for 15 min sliding duration. While the accumulated wear rate after (60 min) was $(150.73 \times 10^{-7}) \text{ mm}^3.\text{mm}^{-1}$ which proves the good wear resistance of the CCMA samples fabricated by PMR due to their low measured values.

The main wear mechanism was adhesive type detected by material transfer, and lower contribution of abrasive type revealed from the existence of fine grooves and no evidence was observed about formation of large longitudinal and transverse cracks which are also proved the good resistance of the CCMA samples to wear. Oxidation and plastic deformation features are observed from the appearance of the worn surface slide when (25 N) was applied. Thin platelet with irregular edges debris particles creation when (25 N) was applied with front face (F) simulating the worn surface features and with ruptured like the configuration of the rare (R) face. The size of the debris particle was around (50 μm) and others with lower size were formed under the maximum test load. While the thickness of them was less than ($\sim 10\mu\text{m}$). These formed debris features reveal the partial uprooted CCMA particles which in turn show the durability of the tested samples against dry sliding under selected parameters.

5. References

- [1] D. Markov and D. Kelly, 2000 " Mechanisms of adhesion-initiated catastrophic wear: pure sliding", *Wear* **239**. 189–210.
- [2] William Murphy, Jonathan Black and Garth Hastings, "*Handbook of Biomaterial Properties*", Published by Chapman & Hall, Second Edition, Springer Science+Business Media New York 2016, p. 487.
- [3] Hendra Hermawan, Dadan Ramdan and Joy R. P. Djuansjah 2011 *Metals for Biomedical Applications, Biomedical Engineering-From Theory to Applications*, Prof. Reza Fazel (Ed.),

- InTech, p.421. Available from: <http://www.intechopen.com/books/biomedical-engineering-from-theory-to-applications/metals-for-biomedical-applications>.
- [4] Mitsuo Niinomi, 2002 "Recent Metallic Materials for Biomedical Applications". *Metal. Mater. Transac. A*, **33 A**, pp.477-486.
 - [5] Mohamed A. Hussein, Abdul Samad Mohammed, and Naser Al-Aqeeli, 2015 "Wear Characteristics of Metallic Biomaterials: A Review", *Materials*, **8**, pp.2749-2768.
 - [6] Qingliang Wang, Chuanhui Huang and Lei Zhang, 2012 "Microstructure and Tribological Properties of Plasma Nitriding Cast CoCrMo Alloy", *J. Mater. Sci. Technol.*, **28**(1), pp.60-66.
 - [7] Y. Bedolla-Gil and M.A.L. Hernandez-Rodriguez, 2013 "Tribological Behavior of a Heat-Treated Cobalt-Based Alloy", *Journal of Materials Engineering and Performance*, **22**(2), pp. 541-547.
 - [8] Kenneth R. St. John, Lyle D. Zardiackas and Robert A. Poggie, 2004 "Wear Evaluation of Cobalt-Chromium Alloy for Use in a Metal-on-Metal Hip Prosthesis", *J Biomed Mater Res Part B: Appl Biomater*, **68B**, pp.1-14.
 - [9] Akihiko Chiba, Kazushige Kumagai, Naoyuki Nomura, and Satoru Miyakawa, 2007 "Pin-on-disk wear behavior in a like-on-like configuration in a biological environment of high carbon cast and low carbon forged Co-29Cr-6Mo alloys," *Acta Materialia*, vol. **55**, pp.1309-1318.
 - [10] R Varano, J D Bobyn, J B Medley, and S Yue, 2006 "The effect of microstructure on the wear of cobalt-based alloys used in metal-on-metal hip implants," *Proc. IMechE Part H: J. Engineering in Medicine*, Vol. **220**, pp. 145-159.
 - [11] C. Zhao, J. Zhou, Q. Mei and F. Ren, 2018 Microstructure and dry sliding wear behavior of ultrafine-grained Co-30at% Cr alloy at room and elevated temperatures, *Journal of Alloys and Compounds*, pp1-33.
 - [12] A. J. Saldívar-García and H. F. Lo'pez, 2005 "Microstructural effects on the wear resistance of wrought and as-cast Co-Cr-Mo-C implant alloys", *Biomed Mater Res* **74A**, pp.269-274.
 - [13] Dong Mua, Bao-luo Shen and Xin Zhao, 2010 "Effects of boronizing on mechanical and dry-sliding wear properties of CoCrMo alloy", *Materials and Design* **31**, pp.3933-3936.
 - [14] Chi-Wai Chan, Graham C. Smith and Seunghwan Lee, 2018 "A Preliminary Study to Enhance the Tribological performance of CoCrMo Alloy by Fibre Laser Remelting for Articular Joint Implant Applications", *Lubricants*, pp.1-17.
 - [15] Ali Hobi Haleem, Haydar H.J., Jamal Al-Deen and Ammar H. Khilfa, 2016 Studying the Properties of CoCrMo Alloys (F75) Doped Ge Using (Powder Metallurgy) Technique, *Journal of Babylon University/Engineering Sciences*, Vol.**24**(3), pp 723-729.
 - [16] Nikhilesh Chawla and Krishan K. Chawla, 2006 "Metal Matrix Composites" *Library of Congress Cataloging in Publication Data* © Springer Science Business Media, p340.
 - [17] Hani Aziz Ameen, Khairia Salman Hassan and Ethar Mohamed Mhdi Mubarak, 2011 "Effect of loads, sliding speeds and times on the wear rate for different materials", *Am. J. Sci. Ind. Res.*, **2**(1), pp. 99-106.
 - [18] M. Dourandish, D. Godlinski, A. Simchi and V. Firouzdor, 2008 "Sintering of biocompatible P/M Co-Cr-Mo alloy (F-75) for fabrication of porosity-graded composite structures", *Materials Science and Engineering A*, **472**, pp. 338-346.
 - [19] G. Turner and P.H. Holoway, 1992 "Oxidation of Polycrystalline Chromium Between 30°C and 400°C", *Acta Physica Polonica A*, Vol. **81**, PP.273-283.
 - [20] Amit Aherwar, Amit Singh and Amar Patnaik, 2016 "Study on mechanical and wear characterization of novel Co30Cr4Mo biomedical alloy with added nickel under dry and wet sliding conditions using Taguchi approach", *Proc IMechE Part L: J Materials: Design and Applications*, **0**(0), pp1-20.
 - [21] R. Varano, J. D. Bobyn, J. B. Medley and S. Yue1, 2006 "Effect of Microstructure on the Dry Sliding Friction Behavior of CoCrMo Alloys Used in Metal-On-Metal Hip Implants", *J Biomed Mater Res Part B: Appl Biomater* **76B**, pp. 281-286.
 - [22] Z. Doni, A.C. Alves, F. Toptan, J.R. Gomes, A. Ramalho, M. Buciumeanu, L. Palaghian and F.S. Silva, 2013 "Dry sliding and tribocorrosion behaviour of hot pressed CoCrMo biomedical alloy as compared with the cast CoCrMo and Ti6Al4V alloys ", *Materials and Design* **52**, pp.47-57.

- [23] E. Atar, 2013 “Sliding wear performances of 316 L, Ti6Al4V, and CoCrMo alloys”, *Kovove Mater.* **51**, pp.183-188.
- [24] S. Affatato, M. Spinelli, M. Zavalloni, C. Mazzega-Fabbro and M. Viceconti, 2008 “Review: Tribology and total hip joint replacement: Current concepts in mechanical simulation”, *Medical Engineering & Physics* **30**, pp.1305-1317.